Basolateral anion transport mechanisms underlying fluid secretion by mouse, rat and guinea-pig pancreatic ducts

M. Paz Fernández-Salazar[1], Patricia Pascua[1], José Julián Calvo[1], María A. López[1], R. Maynard Case[2], Martin C. Steward[2] and José I. San Román[1]

[1] *Departamento de Fisiología y Farmacología, Universidad de Salamanca, 37007 Salamanca, Spain*
[2] *School of Biological Sciences, University of Manchester, Manchester M13 9PT, UK*

Fluid secretion by interlobular pancreatic ducts was determined by using video microscopy to measure the rate of swelling of isolated duct segments that had sealed following overnight culture. The aim was to compare the HCO_3^- requirement for secretin-evoked secretion in mouse, rat and guinea-pig pancreas. In mouse and rat ducts, fluid secretion could be evoked by 10 nM secretin and 5 μM forskolin in the absence of extracellular HCO_3^-. In guinea-pig ducts, however, fluid secretion was totally dependent on HCO_3^-. Forskolin-stimulated fluid secretion by mouse and rat ducts in the absence of HCO_3^- was dependent on extracellular Cl^- and was completely inhibited by bumetanide (30 μM). It was therefore probably mediated by a basolateral Na^+–K^+–$2Cl^-$ cotransporter. In the presence of HCO_3^-, forskolin-stimulated fluid secretion was reduced ~40% by bumetanide, ~50% by inhibitors of basolateral HCO_3^- uptake (3 μM EIPA and 500 μM H_2DIDS), and was totally abolished by simultaneous application of all three inhibitors. We conclude that the driving force for secretin-evoked fluid secretion by mouse and rat ducts is provided by parallel basolateral mechanisms: Na^+–H^+ exchange and Na^+–HCO_3^- cotransport mediating HCO_3^- uptake, and Na^+–K^+–$2Cl^-$ cotransport mediating Cl^- uptake. The absence or inactivity of the Cl^- uptake pathway in the guinea-pig pancreatic ducts may help to account for the much higher concentrations of HCO_3^- secreted in this species.

(Resubmitted 22 January 2004; accepted after revision 12 February 2004; first published online 20 February 2004)
Corresponding author J. I. San Román: Departamento de Fisiología y Farmacología, Universidad de Salamanca, Edificio Departamental, Campus Miguel de Unamuno, 37007 Salamanca, Spain. Email: nachosr@usal.es

There are significant variations in the pattern of pancreatic electrolyte secretion between different species, particularly in the concentrations of the principal anions, Cl^- and HCO_3^-. Following stimulation with the hormone secretin, the pancreas of the guinea-pig secretes HCO_3^- ions at a final concentration of up to 150 mM and secretes relatively little Cl^- (Padfield *et al.* 1989). The same appears to be true in the human, cat and dog (Case & Argent, 1993). In the rat, however, the secreted HCO_3^- concentration never exceeds about 70 mM and there is a substantial secretion of Cl^- ions (Sewell & Young, 1975). In the mouse, the HCO_3^- concentration may be even lower (Mangos *et al.* 1973). Since secretin-evoked secretion in all of these species is believed to derive mainly from the ductal system, the differences in anion output may reflect important species differences in the transport mechanisms operating in the ductal epithelium.

No major species differences have yet been identified in the pathways available for Cl^- and HCO_3^- efflux across the luminal membrane. Both the cystic fibrosis transmembrane conductance regulator (CFTR) and a calcium-activated chloride channel (CACC) have been observed in mouse (Gray *et al.* 1994), rat (Ashton *et al.* 1993; Gray *et al.* 1993) and guinea-pig (O'Reilly *et al.* 2000). There is also functional evidence for an anion exchanger in the luminal membrane in mouse (Lee *et al.* 1999), rat (Zhao *et al.* 1994) and guinea-pig (Ishiguro *et al.* 2000) although its molecular identity remains uncertain. Immunohistochemical studies of mouse and human pancreas suggest that the luminal anion exchanger might be a member of the SLC26 family (Lohi *et al.* 2000; Greeley *et al.* 2001). Furthermore, functional studies of SLC26A6, which is strongly expressed in human pancreatic duct cells, indicate that this anion exchanger may be electrogenic (Ko *et al.* 2002; Xie *et al.* 2002) thus potentially facilitating HCO_3^- secretion across the luminal membrane.

Despite the steep HCO_3^- concentration gradient that exists during maximal secretion in the guinea-pig ducts, recent evidence suggests that HCO_3^- secretion across the luminal membrane may be explained by a favourable

 DOI: 10.1113/jphysiol.2004.061762

electrochemical gradient for HCO_3^- efflux (Ishiguro *et al.* 2002*b*) and is probably mediated by an anion channel and/or an electrogenic anion exchanger. If this is true, then it also becomes necessary to explain why the guinea-pig ducts secrete so little Cl^-. CFTR is normally more permeable to Cl^- than to HCO_3^- (Poulsen *et al.* 1994; Linsdell *et al.* 1997; O'Reilly *et al.* 2000), so even a small gradient for Cl^- efflux across the luminal membrane would lead to a significant secretion of this ion.

Measurements of intracellular Cl^- in guinea-pig duct cells show that, during maximal HCO_3^- secretion, the intracellular concentration drops quickly to a low value as a result of Cl^- efflux through the large luminal CFTR conductance and an apparent lack of compensatory Cl^- uptake across the basolateral membrane (Ishiguro *et al.* 2002*a*). The result is that Cl^- approaches electrochemical equilibrium at the luminal membrane. The high concentration of HCO_3^- in the fluid secreted by the guinea-pig ducts may thus be attributed to a lack of driving force for Cl^- secretion rather than any novel mechanism for HCO_3^- transport. On the other hand, for the rat and mouse ducts to produce a mixed secretion of Cl^- and HCO_3^-, there must be pathways for uptake of Cl^- at the basolateral membrane in order to maintain the driving force for Cl^- secretion across the luminal membrane.

In the present study, which is also the first to investigate fluid secretion in mouse ducts, our hypothesis is that the differences in the relative Cl^- and HCO_3^- concentrations in the fluid secreted by the rat, mouse and guinea-pig ducts are due to differences in the basolateral transport mechanisms. As far as we can tell, all of these species achieve HCO_3^- accumulation across the basolateral membrane in the same way. This involves a combination of H^+ extrusion, principally via Na^+–H^+ exchange, and HCO_3^- uptake via Na^+–HCO_3^- cotransport. Pathways for Cl^- uptake in pancreatic duct cells are not so clearly defined. By analogy with other secretory epithelia, the most likely candidate for basolateral Cl^- accumulation would be a Na^+–K^+–$2Cl^-$ cotransporter such as NKCC1. To our knowledge the only published evidence of NKCC1 expression or activity in pancreatic duct cells has been in studies of the human ductal cell lines Capan-1 (Cheng *et al.* 1998) and CFPAC-1 (Shumaker & Soleimani, 1999) and primary cultures of bovine ductal cells (Cotton, 1998). Another possibility is that Cl^- could be taken up in exchange for intracellular HCO_3^- by a basolateral anion exchanger. There is evidence for such a transporter in both rat and guinea-pig ductal cells (Zhao *et al.* 1994; Ishiguro *et al.* 2000).

The aim of this study was therefore to compare the basolateral transport mechanisms involved in ductal fluid secretion in mouse, rat and guinea-pig pancreas. To do this we have estimated fluid secretory rates from the rate of swelling of sealed interlobular duct segments measured by video microscopy. Our approach has been to explore the sensitivity of secretin- and forskolin-evoked fluid secretion to inhibitors of known basolateral anion transporters in the presence and absence of HCO_3^-. In particular we have sought evidence for the capacity of the ducts to secrete fluid in the absence of HCO_3^- and have examined the effects of the NKCC1 inhibitor bumetanide.

Methods

Animals and materials

All procedures were in accordance with local and national guidelines. Male CD1 mice (16–20 g) and male Wistar rats (250–300 g) were obtained from the University of Salamanca animal breeding facility, and male tri-colour guinea-pigs (375–425 g) from Leeds University. All animals were killed by cervical dislocation.

Secretin, bumetanide, amiloride, 5-(*N*-ethyl-*N*-isopropyl)amiloride (EIPA), 4,4′-diisothiocyanatostilbene-2,2′-disulphonic acid (DIDS), Dulbecco's modified Eagle's medium (DMEM), McCoy's 5A medium, hyaluronidase, soybean trypsin inhibitor (SBTI), *N*-methyl-D-glucamine ($NMDG^+$), sodium glucuronate and bovine serum albumin (BSA) were from Sigma. Forskolin was from Tocris Cookson (Bristol, UK). 2′,7′-bis-(2-carboxyethyl)-5(6)-carboxyfluorescein acetoxymethyl ester (BCECF-AM) and dihydro-4,4′-diisothiocyanato-stilbene-2,2′-disulphonic acid (H_2DIDS) were from Molecular Probes Europe (Leiden, the Netherlands). Purified collagenase (type CLSPA) was from Worthington Biochemical Corporation (Lakewood, NJ, USA). Fetal calf serum and L-glutamine were from Gibco (Invitrogen, Paisley, UK). Cell-Tak was from Becton Dickinson Labware (Bedford, MA, USA). All other chemicals were of high purity grade.

Solutions

The standard Hepes-buffered solution contained (mM): 130 NaCl, 5 KCl, 1 $CaCl_2$, 1 $MgCl_2$, 10 D-glucose and 10 Hepes, and was equilibrated with 100% O_2. The standard HCO_3^--buffered solution contained (mM): 115 NaCl, 25 $NaHCO_3$, 5 KCl, 1 $CaCl_2$, 1 $MgCl_2$, 10 D-glucose, and was equilibrated with 95% O_2–5% CO_2. All solutions were adjusted to pH 7.4 at 37°C. In the NH_4^+ pulse experiments, 20 mM NaCl was replaced with NH_4Cl. The Na^+-free

solutions contained *N*-methyl-D-glucamine ($NMDG^+$) in place of Na^+, and glucuronate replaced Cl^- in the Cl^--free solutions. Concentrated stock solutions of BCECF-AM, forskolin, bumetanide, amiloride, EIPA and DIDS were prepared in dimethylsulfoxide, the final concentration of which did not exceed 0.3% in the experimental solutions.

Isolation and culture of interlobular ducts

Interlobular ducts were isolated from mouse, rat and guinea-pig pancreas following methods previously described for the guinea-pig (Ishiguro *et al.* 1996). Briefly, the pancreas was removed (pooled from two animals in the case of the mouse) and injected with 4 ml of a digestion buffer consisting of DMEM containing 40 U ml^{-1} collagenase, 400 U ml^{-1} hyaluronidase, 0.2 mg ml^{-1} SBTI and 2 mg ml^{-1} BSA. The tissue was chopped with scissors, gassed with 5% CO_2–95% O_2 and incubated at 37°C for 20 min (mouse), 25 min (rat) or 40 min (guinea-pig), and then in 4 ml of fresh digestion buffer for a further 15 min (mouse), 20 min (rat) or 30 min (guinea-pig). The digested tissue was washed with DMEM and resuspended in DMEM containing 0.2 mg ml^{-1} SBTI and 30 mg ml^{-1} BSA. Interlobular ducts were microdissected from samples of tissue suspension under a dissecting microscope using 25-gauge needles, and transferred to McCoy's 5A tissue culture medium supplemented with 10% (v/v) fetal calf serum, 2 mM L-glutamine, 0.15 mg ml^{-1} SBTI, 0.1 I.U. ml^{-1} insulin and 4 μg ml^{-1} dexamethasone. They were cultured at 37°C in 5% CO_2 in air for up to 24 h. During overnight culture, the ends of the ducts usually became sealed, leading to a slow dilatation of the duct lumen.

Measurement of fluid secretion

Ducts were allowed to attach to coverslips pretreated with Cell-Tak (Becton-Dickinson, Bedford, MA, USA) and mounted on the base of a slot-shaped Perspex perfusion chamber with a volume of 220 μl. The chamber was perfused at 1.5 ml min^{-1} with standard Hepes- or HCO_3^--buffered solutions and maintained at 37°C. The isolated ducts, typically 0.3–0.6 mm in length and 50–100 μm in diameter, were visualized at low magnification using an inverted microscope (TMS-F, Nikon or DMIRB, Leica). Bright-field images were acquired at set time intervals using a CCD camera (902A, Watec Corp., Las Vegas, NV, USA) coupled to a PC frame-grabber board (LG-3, Scion Corp., Frederick, MD, USA).

At the end of each experiment the chamber was perfused with a hypotonic solution (the standard Hepes-buffered solution diluted 30% with distilled water) in order to evoke osmotic swelling of the luminal space and thus to confirm that the ends of the duct were completely sealed. Data were discarded from the few ducts (generally less than 5%) that did not show a normal swelling response to the hypotonic challenge.

Scion Image software (Scion Corp, Frederick, MD, USA) was used to analyse the duct images. They were first converted to binary images using a threshold function in which the value selected for the threshold pixel intensity was fixed for the entire series of images. The binary images were then subjected to an automated particle analysis routine, which identified regions of connected pixel elements exceeding a preset minimum size and returned a value for the area of the particles corresponding to the ducts. To correct for the area corresponding to the wall of the ducts, the magnitude of this component was estimated from a manual measurement of the luminal area in the first image of each series using a graphics tablet (Artpad II, Wacom GmbH, Neuss, Germany) and subtracted from each of the area measurements generated automatically for the rest of the series.

Luminal area measurements from individual images were normalized to the average of the first few images in the series thus giving values for the relative area. These were then converted to relative volumes assuming that the duct lumen is approximated by a cylinder. Secretory rate was calculated from the rate of increase in relative volume. Full details of these calculations are given in the Appendix. To obtain absolute values, normalized to the luminal surface area of the epithelium and expressed in pl min^{-1} mm^{-2}, the initial length and area of the luminal space were first converted from pixel values to absolute values using a calibration factor obtained from measurements of a graticule.

Measurement of intracellular pH

Intracellular pH (pH_i) was measured in mouse ducts by microfluorometry as described in detail elsewhere (Ishiguro *et al.* 1996). Briefly, ducts were loaded with the pH-sensitive fluoroprobe BCECF by incubation with 1 μM BCECF-AM for 30 min at room temperature in the Hepes-buffered solution. Ducts were allowed to attach to a Cell-Tak coated coverslip at the base of a 200 μl Perspex perfusion chamber mounted on the stage of a Nikon Diaphot TMD inverted microscope. The chamber was perfused at 1.5 ml min^{-1} and the temperature maintained at 37°C. A small region of the ductal epithelium was illuminated alternately at 440 and 490 nm and the fluorescence was measured at 530 nm. The fluorescence intensities (F_{440} and F_{490}) were each averaged over a 1 s

Table 1. Initial dimensions of interlobular ducts isolated from pancreas of mouse, rat and guinea-pig

	Mouse	Rat	Guinea-pig
Diameter (μm)	59 ± 25	90 ± 31	89 ± 37
Length (μm)	409 ± 117	384 ± 95	459 ± 127
Volume (nl)	0.92 (1.25)	2.04 (2.33)	2.45 (3.66)
Epithelial area (mm^2)	0.078 ± 0.044	0.112 ± 0.058	0.134 ± 0.078
n	508	251	401

Data are means ± S.D. with the exception of the duct volumes, which deviated significantly from a normal distribution and are therefore presented as median values (and interquartile range). Dimensions refer to the diameter, length and volume of the luminal space following overnight culture.

period and repeated at 5 s intervals. Intracellular pH was calculated from the F_{490}/F_{440} ratio using calibration data obtained with the nigericin-K^+ method (Thomas *et al.* 1979).

Statistical analysis

Unless otherwise indicated, data are presented as means ± S.E.M. where the value of *n* quoted is the total number of ducts. Since several ducts were usually imaged together in the video microscopy experiments, we also indicate the number of separate experiments in the figure legends. Unpaired Student's *t* tests were used for the statistical comparison of data; $P < 0.05$ was chosen as the limit for statistical significance.

Results

The majority of the ducts isolated from all three species swelled during the overnight culture period. This occurred as a result of the ends of the ducts sealing and it presumably reflects a slow secretion into the closed luminal space. In general, the sealing occurred slightly less consistently in mice compared with guinea-pigs and rats. Interlobular ducts isolated from mouse pancreas had a similar morphology to those from rats and guinea-pigs although their diameter was significantly smaller. Table 1 shows average dimensions of ducts from all three species.

Stimulation of fluid secretion in mouse pancreatic ducts by secretin and forskolin

Little, if any, spontaneous secretion was observed in unstimulated mouse pancreatic ducts (control, Fig. 1). The secretory rate, calculated from the rate of change in luminal volume, was 14 ± 8 pl min^{-1} mm^{-2} (n = 100) in the Hepes-buffered solution (0–10 min) and 11 ± 6 pl min^{-1} mm^{-2} in the HCO_3^--buffered solution (10–20 min); neither value was significantly different from zero. Upon stimulation with 10 nM secretin in the presence of HCO_3^-, the luminal volume began to increase after a short delay and continued to increase over the following 40 min (secretin, Fig. 1). The initial secretory rate, calculated from the rise in luminal volume over the 30–40 min period, was 95 ± 18 pl min^{-1} mm^{-2} ($n = 10$). This decreased slowly with time, falling to 60 ± 13 pl min^{-1} mm^{-2} over the 50–60 min period.

Direct activation of adenylyl cyclase with 5 μM forskolin was more effective and produced a more sustained secretion (forskolin, Fig. 1), perhaps indicating some down-regulation of secretin receptors during overnight culture. The secretory rate during forskolin stimulation in the presence of HCO_3^- was 260 ± 27 pl min^{-1} mm^{-2} ($n = 26$) over the 30–40 min period and 267 ± 32 pl min^{-1} mm^{-2} over the 50–60 min period.

Fluid secretion in mouse pancreatic ducts in the absence of HCO_3^-

Both secretin and forskolin, when applied during superfusion with the Hepes-buffered solution, i.e. in the nominal absence of HCO_3^-, elicited a clear stimulation of fluid secretion in the mouse pancreatic ducts (Fig. 2*A*). The secretory rates over the 30–60 min period were 64 ± 17 pl min^{-1} mm^{-2} ($n = 9$) and 126 ± 22 pl min^{-1} mm^{-2} ($n = 12$) in secretin- and forskolin-stimulated ducts, respectively.

This observation was surprising given that ducts isolated from the guinea-pig pancreas do not respond to forskolin and secretin unless HCO_3^- is present in the extracellular medium. This is shown in Fig. 2*B* where guinea-pig ducts were stimulated first with forskolin in the absence of HCO_3^-. The secretory rate was not significantly different from zero (5 ± 38 pl min^{-1} mm^{-2}, $n = 10$) until HCO_3^- was introduced into the bath at 20 min whereupon it increased rapidly to 774 ± 116 pl min^{-1} mm^{-2}. We have shown previously that this is because fluid secretion in guinea-pig ducts is coupled exclusively to transepithelial HCO_3^- transport (Ishiguro *et al.* 1998). Unstimulated guinea-pig ducts (Fig. 2*B*) also showed a significant HCO_3^--dependent spontaneous secretion (241 ± 70 pl min^{-1} mm^{-2}, $n = 22$).

Effects of bumetanide on fluid secretion in mouse ducts

Since mouse pancreatic ducts are able to secrete fluid in the absence of HCO_3^-, they are presumably able to secrete

another anion. In these experiments this was most likely to be Cl^- as it was the only other anion present in the Hepes-buffered solution apart from Hepes itself. This was confirmed by experiments in which Cl^- was completely replaced by glucuronate (data not shown). Ducts were first incubated for 40 min in the Cl^--free, Hepes-buffered solution and then stimulated with forskolin. In the absence of Cl^- there was no basal secretion and no response to forskolin.

To test the hypothesis that the secretion of Cl^- ions might be driven by a basolateral Na^+–K^+–$2Cl^-$ cotransporter, we examined the effect of the cotransport inhibitor bumetanide (Fig. 3). Bumetanide (30 μM), completely blocked forskolin-evoked fluid secretion in the absence of extracellular HCO_3^-, i.e. during superfusion with the Hepes-buffered solution. This was true both when bumetanide was applied 20 min after the onset of stimulation (Fig. 3*A*) and when forskolin was applied in the continuous presence of bumetanide (Fig. 3*B*).

In the experiment shown in Fig. 3*B*, HCO_3^- was subsequently introduced into the bath at 30 min. In the absence of bumetanide, the introduction of HCO_3^- led to a sustained increase in the secretory rate. When bumetanide was present, HCO_3^- induced an initially brisk secretion that was quickly followed by a decline in secretory rate and then a slower increase. After 20 min, however, a steady rate had been attained which was not significantly different from that measured in the absence of bumetanide at the equivalent time point.

The calculated secretory rates, which are summarized in Fig. 3*C*, support the hypothesis that, in the absence of extracellular HCO_3^-, fluid secretion is coupled to Cl^- transport via a bumetanide-sensitive Na^+–K^+–$2Cl^-$ cotransporter, most probably NKCC1. In the presence of extracellular HCO_3^-, however, the secretory rate at steady state was little affected by inhibition of the cotransporter.

Effects of bumetanide on fluid secretion in rat ducts

In view of the interesting results obtained with mouse pancreatic ducts, we repeated the experiments using ducts

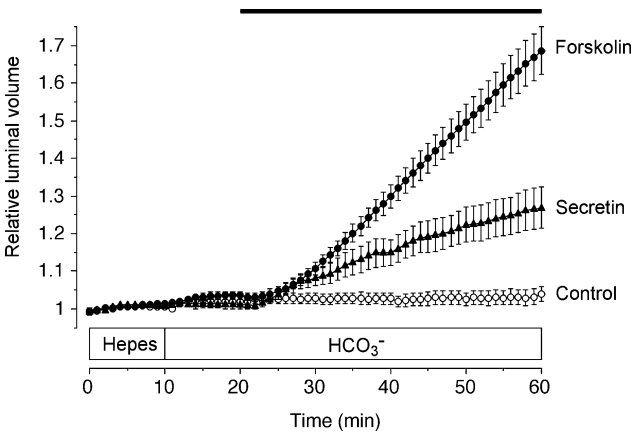

Figure 1. Changes in relative luminal volume of mouse pancreatic ducts stimulated with secretin and forskolin
Mouse ducts superfused first with the Hepes-buffered solution were switched at 10 min to the HCO_3^--buffered solution for the remainder of the experiment. From 20 min the ducts were exposed either to no agonist (○, $n = 64$ in 9 experiments), to 10 nM secretin (▲, $n = 10$ in 5 experiments) or to 5 μM forskolin (●, $n = 26$ in 10 experiments) as indicated by the horizontal bar. Data are means ± S.E.M. of n values. The secretory rates given in the text were calculated from the rates of increase in relative luminal volume.

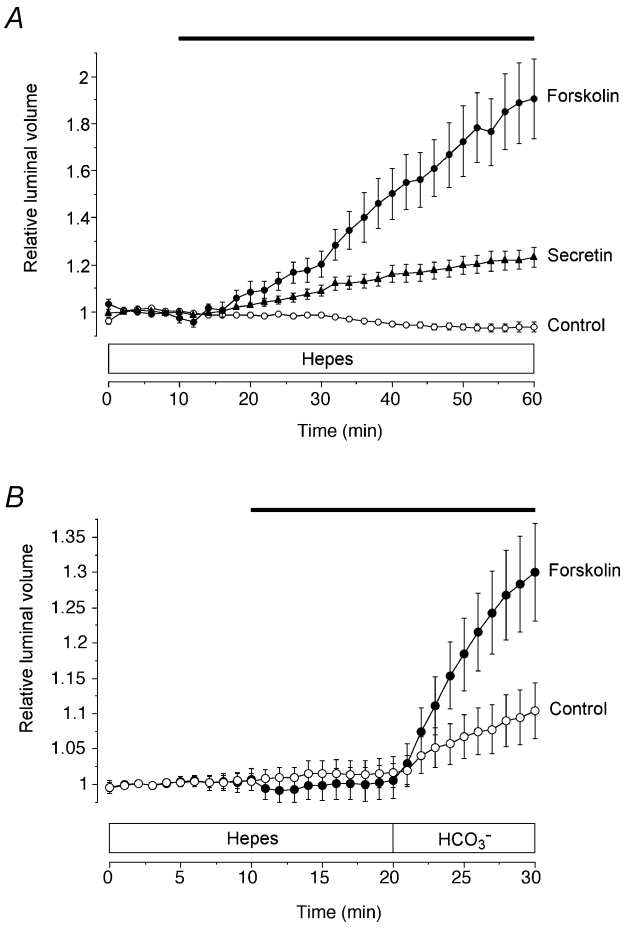

Figure 2. Fluid secretion by mouse and guinea-pig pancreatic ducts in the nominal absence of extracellular HCO_3^-
A, mouse ducts superfused throughout with the Hepes-buffered solution and exposed either to no agonist (○, $n = 4$ in 3 experiments), to 10 nM secretin (▲, $n = 9$ in 6 experiments) or to 5 μM forskolin (●, $n = 12$ in 8 experiments) as indicated by the horizontal bar. *B*, guinea-pig ducts superfused first with the Hepes-buffered solution and then with the HCO_3^--buffered solution, and exposed either to no agonist (○, $n = 22$ in 8 experiments) or to 5 μM forskolin as indicated by the horizontal bar (●, $n = 10$ in 4 experiments).

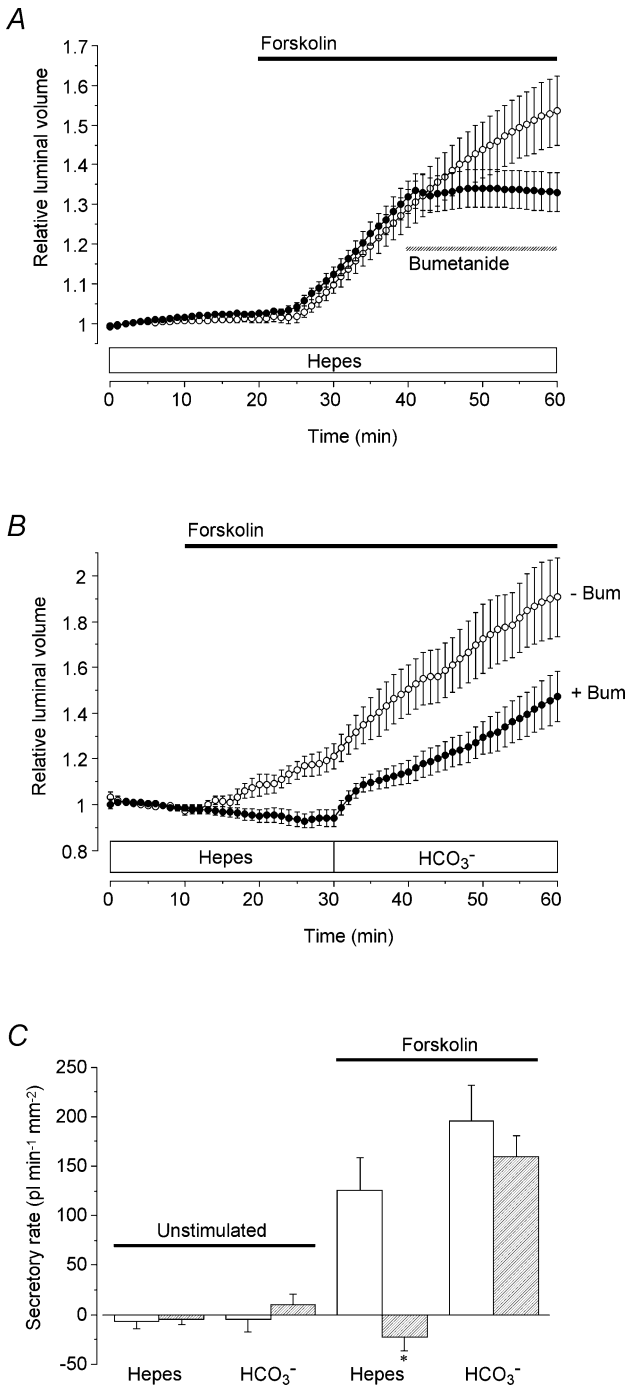

Figure 3. Effect of bumetanide on fluid secretion by mouse pancreatic ducts in the presence or absence of HCO_3^-
A, mouse ducts superfused throughout with the Hepes-buffered solution. From 20 min the ducts were stimulated with 5 μM forskolin (filled horizontal bar) and from 40 to 60 min they were exposed either to no blocker (○, $n = 15$ in 4 experiments) or to 30 μM bumetanide (●, $n = 20$ in 7 experiments) as indicated by the hatched horizontal bar. *B*, mouse ducts switched from the Hepes- to the HCO_3^--buffered solution at 30 min. From 10 min the ducts were stimulated with 5 μM forskolin (horizontal bar). Ducts were superfused either in the absence (○, $n = 17$ in 8 experiments) or in the continuous presence of 30 μM bumetanide (bum) (●, $n = 11$ in 6 experiments). *C*, mean secretory rates calculated from the data shown in Fig. 3*B* in ducts stimulated with 5 μM forskolin compared with equivalent control data obtained in unstimulated ducts (not shown; $n = 12$ in 4 experiments in the absence of bumetanide; $n = 15$ in 3 experiments in the presence of bumetanide). Secretory rates in the Hepes- and HCO_3^--buffered solutions were estimated over the 20–30 min and 50–60 min periods, respectively. Open bars represent values obtained in the absence of bumetanide, and hatched bars represent values obtained in ducts continuously superfused with 30 μM bumetanide. Secretory rates that in the presence of bumetanide were judged significantly different from the corresponding control values by unpaired Student's *t* test are indicated by an asterisk.

isolated from rat pancreas. Secretin-evoked fluid secretion by rat ducts has previously been reported to be dependent on HCO_3^- (Argent *et al.* 1986).

There was little or no spontaneous secretion in the rat ducts under the conditions of our experiments, but surprisingly both secretin (10 nM) and forskolin (5 μM) evoked a brisk secretion in the absence of extracellular HCO_3^- (Fig. 4*A* and *B*). Under these conditions, the rate of forskolin-evoked secretion by the rat ducts (200 ± 38 pl min^{-1} mm^{-2}; $n = 14$) was greater than that by the mouse ducts (124 ± 28 pl min^{-1} mm^{-2}). However, the secretory rate after switching to the HCO_3^--buffered perfusate (217 ± 34 pl min^{-1} mm^{-2}) was similar to that observed in the mouse ducts under identical conditions (242 ± 37 pl min^{-1} mm^{-2}).

As in the mouse ducts, bumetanide completely blocked forskolin-evoked secretion in the absence of HCO_3^- but had little effect in the presence of HCO_3^- (Fig. 4*B*). When HCO_3^- was first introduced into the bath at 30 min the secretory rate in the presence of bumetanide initially exceeded that at the equivalent time point in the control experiments. After a further 10 min, however, there was no significant difference between the two. The effects of bumetanide on secretion in the presence and absence of HCO_3^- are summarized in Fig. 4*C*.

Inhibition of basolateral HCO_3^- transporters in mouse ducts

Our next objective was to estimate the relative contributions of HCO_3^- and Cl^- transport to fluid secretion in mouse and rat pancreatic ducts under approximately physiological conditions, i.e. with 125 mM Cl^- and 25 mM HCO_3^- in the extracellular fluid. According to our results, Cl^- secretion is probably driven by a basolateral Na^+–K^+–$2Cl^-$ cotransporter and this

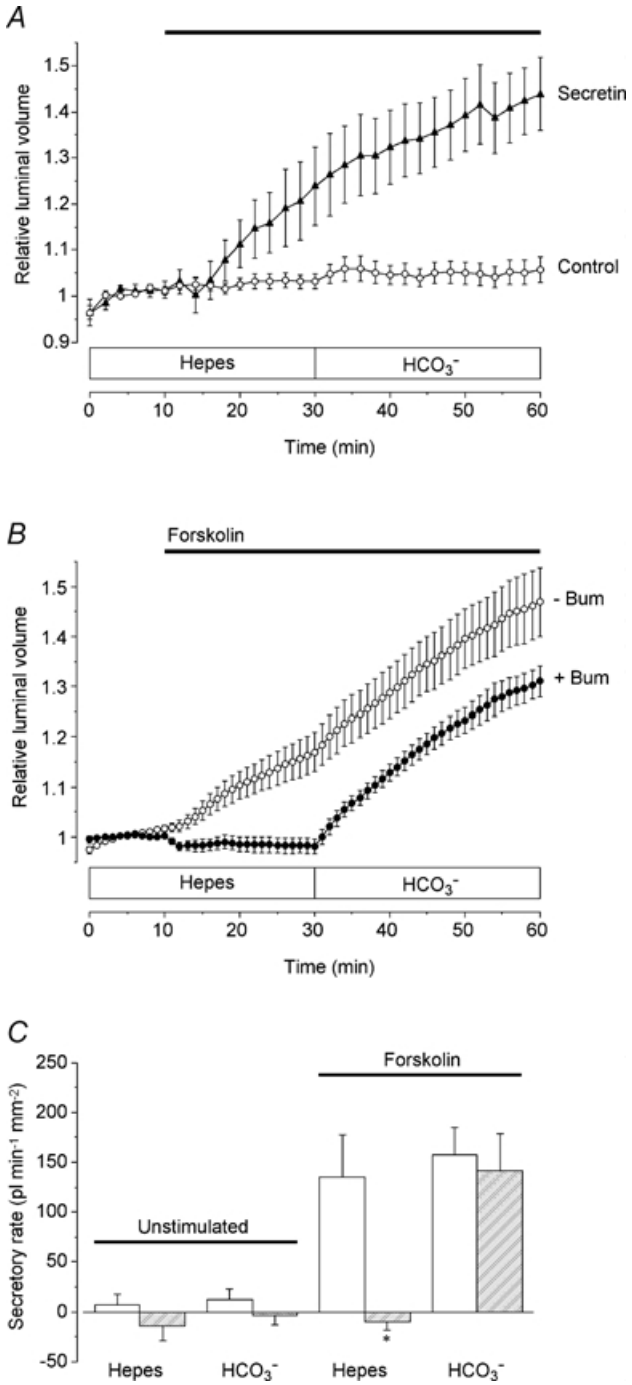

Figure 4. HCO_3^- dependence and bumetanide sensitivity of fluid secretion by rat pancreatic ducts

A, rat ducts superfused initially with the Hepes-buffered solution and after 30 min with the HCO_3^--buffered solution. From 10 min the ducts were exposed either to no agonist (○, $n = 17$ in 4 experiments) or to 10 nM secretin (▲, $n = 10$ in 4 experiments) as indicated by the horizontal bar. *B*, rat ducts superfused initially with the Hepes-buffered solution and after 30 min with the HCO_3^--buffered solution. From 10 min the ducts were exposed to 5 μM forskolin (horizontal bar), either in the absence (○, $n = 14$ in 4 experiments) or in the continuous presence of 30 μM bumetanide (bum) (●, $n = 15$ in 4 experiments). *C*, mean secretory rates calculated from the data shown in Fig. 4*B* in ducts stimulated with 5 μM forskolin compared with equivalent control data obtained in unstimulated ducts (not shown; $n = 15$ in 3 and 17 in 4 in the presence and absence of bumetanide, respectively). Secretory rates in the Hepes- and HCO_3^--buffered solutions were estimated over the 20–30 min and 50–60 min periods, respectively. Open bars represent values obtained in the absence of bumetanide, and hatched bars represent values obtained in ducts continuously superfused with 30 μM bumetanide. Secretory rates that in the presence of bumetanide were judged significantly different from the corresponding control values by unpaired Student's *t* test are indicated by an asterisk.

component can be completely inhibited by bumetanide. According to the current model for HCO_3^- secretion, accumulation of HCO_3^- occurs through the activity of a basolateral Na^+–H^+ exchanger (NHE1) and a Na^+–HCO_3^- cotransporter (NBC1) (Zhao *et al.* 1994; Ishiguro *et al.* 1996; Sohma *et al.* 2000). Thus it should be possible to block HCO_3^- secretion by application of amiloride, an inhibitor of NHE1, and DIDS, an inhibitor of NBC1. We therefore expected to obtain some indication of the relative contributions of the two mechanisms by examining the effects of amiloride and DIDS, with and without bumetanide, on secretory rate during stimulation with 5 μM forskolin.

Under these conditions, i.e. in the presence of HCO_3^-, combined application of amiloride, DIDS and bumetanide would be expected to completely abolish forskolin-stimulated fluid secretion. However, using amiloride and DIDS at concentrations (300 μM and 100 μM, respectively) previously found to be effective in blocking HCO_3^- uptake in guinea-pig ducts (Szalmay *et al.* 2001; Hegyi *et al.* 2003), we did not observe a complete inhibition of fluid secretion in the mouse ducts (Fig. 5). This result could indicate the existence of an additional basolateral transport pathway or could be due to incomplete block of the NHE1 and/or NBC1 in this species. To address the latter possibility, we used measurements of intracellular pH to test the effects of these concentrations of amiloride and DIDS on HCO_3^- accumulation across the basolateral membrane.

Intracellular pH measurements in mouse ductal cells

Basolateral NHE1 and NBC1 activities were evaluated by measuring intracellular pH in mouse duct cells loaded with the pH-sensitive fluoroprobe BCECF and superfused with the HCO_3^--buffered solution. The cells were exposed to a standard acid-loading protocol in which a 2 min pulse of 20 mM NH_4Cl was followed by 5 min exposure to a Na^+-free bath solution. Figure 6*A* shows the resulting changes in pH_i which led to an intracellular acidification of approximately 0.6 pH units. In the absence

of extracellular Na^+, there was no significant recovery of pH_i. However, the recovery was rapid and complete when the extracellular Na^+ was restored, indicating that the acid extrusion and base loading mechanisms in these cells are totally dependent on Na^+.

When extracellular Na^+ was restored in the presence of 300 μM amiloride and 100 μM DIDS (the concentrations used in the fluid secretion measurements shown in Fig. 5) the recovery of pH_i was only partially inhibited (71.5 $\pm$ 9.8%, $n = 5$; Fig. 6*B*) suggesting that these inhibitor concentrations were not as effective as we had presumed. After testing several amiloride and DIDS analogues, we found that 3 μM EIPA and 500 μM H_2DIDS was the most effective combination in inhibiting the recovery of pH_i from acid loading (83.2 $\pm$ 4.7%, $n = 5$; Fig. 6*C*).

Relative contributions of basolateral HCO_3^- and Cl^- transport

When the experiment shown in Fig. 5 was repeated using 30 μM bumetanide, 3 μM EIPA and 500 μM H_2DIDS, fluid secretion in the mouse ducts was now totally abolished (Fig. 7*A*). The mean values for the percentage inhibition of secretion obtained with the inhibitors, applied separately and in combination, are shown in Fig. 7*B* (open bars). In each case, the secretory rate over the 50–60 min time period was compared with the rate from 30 to 40 min, prior to the application of the inhibitors. In the control group,

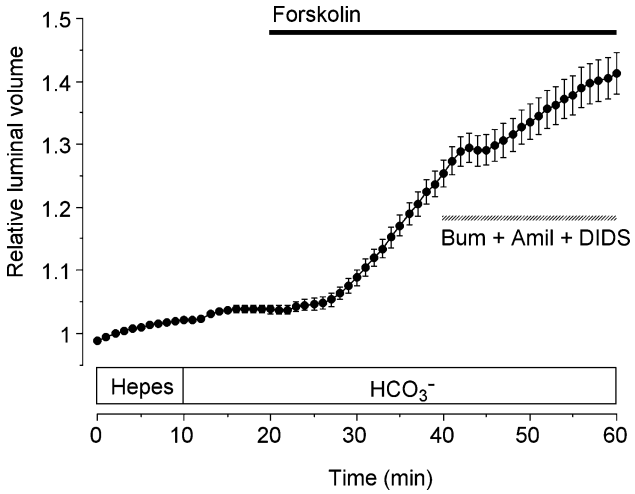

Figure 5. Effects of bumetanide, amiloride and DIDS on fluid secretion by mouse pancreatic ducts
Mouse ducts were stimulated with 5 μM forskolin in the presence of HCO_3^-, as indicated by the filled horizontal bar, and then exposed to 30 μM bumetanide (bum), 300 μM amiloride (amil) and 100 μM DIDS as indicated by the hatched horizontal bar ($n = 26$ in 10 experiments).

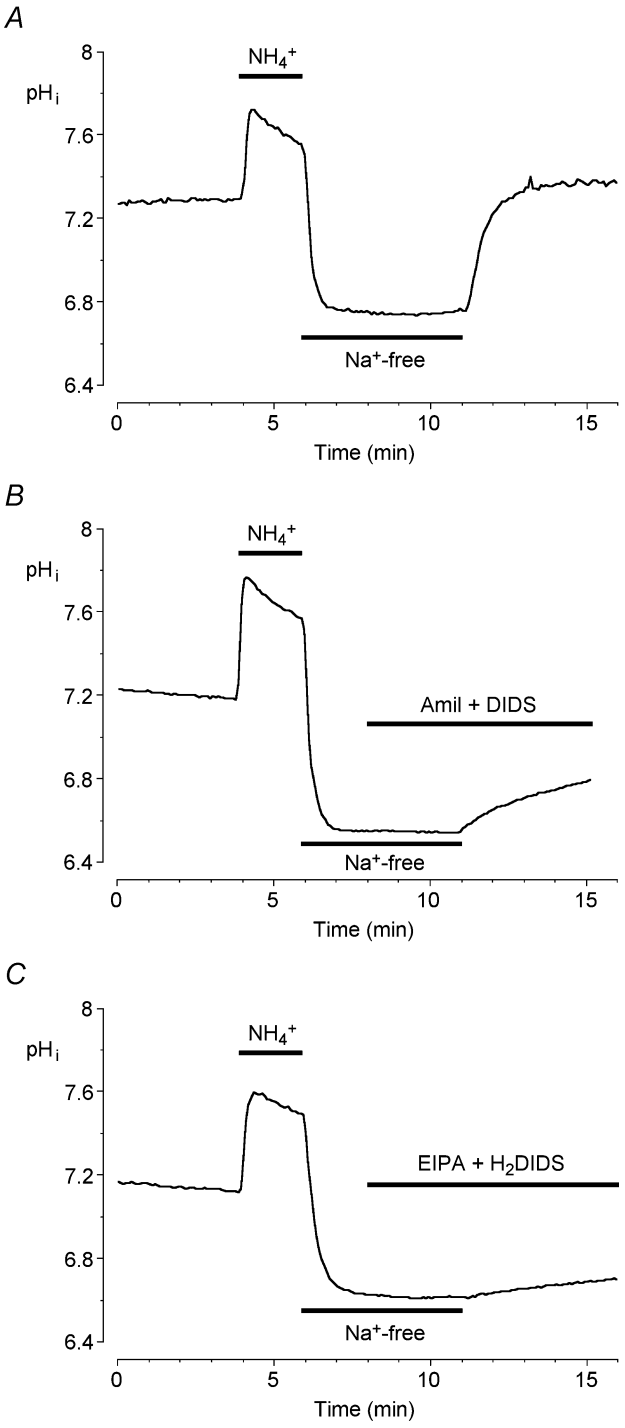

Figure 6. Effects of transport inhibitors on intracellular pH recovery after an acid load in mouse pancreatic ductal cells
Mouse duct cells superfused with the HCO_3^--buffered solution were acid loaded by a brief (2 min) exposure to 20 mM NH_4Cl followed by superfusion with a Na^+-free solution for the following 5 min after which Na^+ was restored. *A*, a representative control experiment performed in the absence of any inhibitors. *B*, pH_i recovery in the presence of 300 μM amiloride (amil) and 100 μM DIDS, which were applied 3 min before Na^+ was restored. *C*, pH_i recovery in the presence of 3 μM EIPA and 500 μM H_2DIDS. Traces are each representative of 5 different experiments.

where no inhibitors were applied, there was no significant change from the 30–40 min to 50–60 min time period.

As judged by the acute effects of the inhibitors, the components of the fluid secretion sensitive to bumetanide and to EIPA + H_2DIDS are quite comparable in magnitude during sustained secretion in the presence of HCO_3^-. Furthermore a similar pattern of inhibition was observed in comparable measurements on rat ducts (hatched bars; Fig. 7*B*). This suggests that Cl^- secretion and HCO_3^- secretion contribute approximately equally to the process of fluid secretion in both mouse and rat ducts.

It should be pointed out that these results appear to be in conflict with those from the experiments described earlier (Figs 3*B* and 4*B*) where the secretory rate in the presence of HCO_3^- reached similar values in the presence and absence of bumetanide. Possible explanations for the discrepancy between the effects of acute and chronic bumetanide treatment are discussed below. However, we were able to confirm that the fluid secretion evoked by the introduction of HCO_3^- during chronic treatment with bumetanide was completely abolished by EIPA + H_2DIDS in both mouse and rat ducts (data not shown). This suggests that the difference between the acute and chronic effects of bumetanide signifies a difference in the relative contributions of the basolateral uptake pathways rather than the appearance of an additional pathway or failure of bumetanide to sustain its inhibitory effect on the Na^+–K^+–2Cl^- cotransporter.

Discussion

This paper presents the first investigation of fluid secretion by interlobular ducts isolated from the mouse pancreas. It reveals that two parallel secretory mechanisms contribute to secretin-evoked fluid secretion in this species. Furthermore, the same two mechanisms also appear to exist in the rat. One depends on the presence of HCO_3^- in the extracellular fluid while the other is independent of HCO_3^-. Because the latter mechanism is inhibited by bumetanide, it probably involves the secretion of Cl^- ions that have entered the cell via a basolateral Na^+–K^+–2Cl^- cotransporter.

Measurement of fluid secretion in isolated ducts

The most direct method for measuring fluid secretion in isolated pancreatic ducts is to collect the secreted fluid by micropuncture (Argent *et al.* 1986). This also allows the measurement of electrolyte concentrations in the secreted fluid and it has provided valuable information about the regulation of fluid secretion in the rat pancreatic duct (Ashton *et al.* 1990, 1991). On the other hand, it only gives a single, average measurement of the secretory rate over a fairly long collection period, typically 1 h, and does not allow acute effects of solution changes to be observed in the same duct.

Because the ends of the isolated ducts seal in culture, it is possible to measure the secretory rate as a function of time by measuring the swelling of the ducts as the lumen

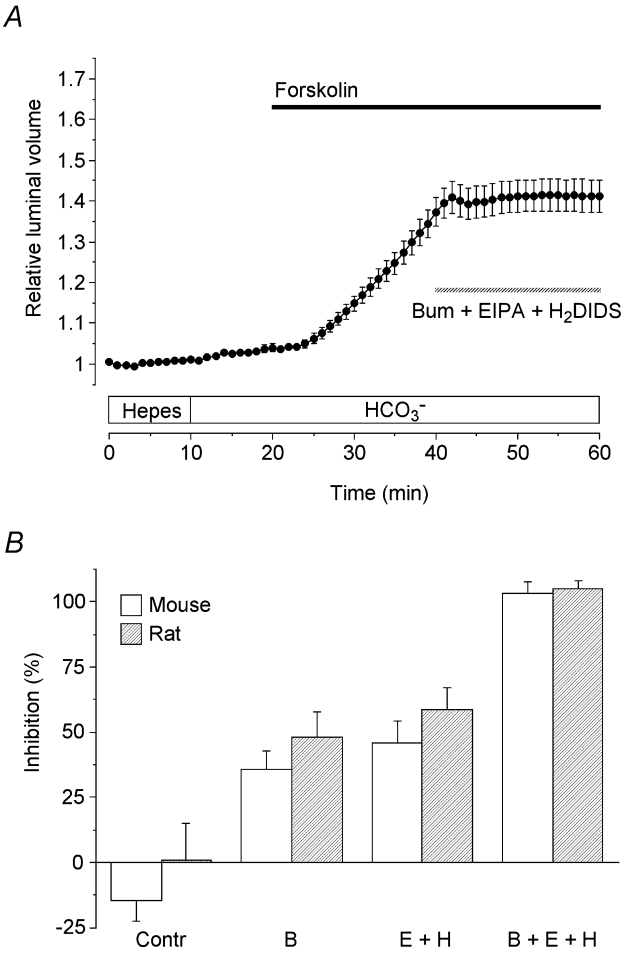

Figure 7. Effects of bumetanide, EIPA and H_2DIDS on fluid secretion by mouse and rat pancreatic ducts

A, mouse ducts were stimulated with 5 μM forskolin in the presence of HCO_3^- (filled horizontal bar) and then exposed to 30 μM bumetanide (bum), 3 μM EIPA and 500 μM H_2DIDS as indicated by the hatched horizontal bar ($n = 40$ in 14 experiments). *B*, percentage inhibition of the secretory rate in mouse ducts (open bars) and rat ducts (hatched bars) in the absence of inhibitors (Contr; mouse $n = 26$ in 10, rat $n = 14$ in 7), in the presence of 30 μM bumetanide (B; mouse $n = 35$ in 11, rat $n = 23$ in 5), in the presence of 3 μM EIPA plus 500 μM H_2DIDS (E + H; mouse $n = 50$ in 14, rat $n = 45$ in 9) and in the presence of all three inhibitors (B + E + H; mouse $n = 40$ in 14, rat $n = 24$ in 8). Values were calculated by comparing secretory rates in the 50–60 min period with those in the 30–40 min period in experiments which all followed the protocol shown in panel *A*.

gradually fills with secreted fluid. This can be done either by fluorescence imaging, using a fluorescent marker injected into the luminal space (Ishiguro *et al.* 1998), or by the simpler bright-field imaging technique described in this paper. As can be seen in several of the figures presented here, stimulated ducts may swell up to twice their initial volume without any significant decline in secretory rate. This indicates that the duct wall is relatively compliant and that any build-up of intraluminal pressure has little effect on the measurements.

The secretory rates that we measured by video microscopy in mouse and rat ducts stimulated with forskolin (242 ± 37 and 217 ± 34 pl min^{-1} mm^{-2}, respectively) were considerably smaller than those observed in guinea-pig ducts under similar conditions (774 ± 116 pl min^{-1} mm^{-2}). This difference appears to be consistent with published values from *in vivo* and perfused preparations of the rat pancreas where the secretory response to secretin is relatively weak compared with guinea-pig, cat, dog and human (Sewell & Young, 1975; Case & Argent, 1993) Unfortunately, no comparable data are available for the mouse pancreas.

Dependence of fluid secretion on HCO_3^-

The observation that the mouse and rat ducts were capable of secreting fluid in the absence of HCO_3^- was surprising given the total dependence of fluid secretion on HCO_3^- transport in the guinea-pig. Furthermore, previous work on rat ducts using the micropuncture technique had shown that secretin-evoked fluid secretion was dependent on HCO_3^- (Argent *et al.* 1986). So too had earlier studies of secretion in the isolated, perfused rat pancreas (Kanno & Yamamoto, 1977; Petersen & Ueda, 1977). While the results from the perfused pancreas studies may have been affected by inappropriate or inadequate buffering of the perfusate in the absence of HCO_3^-, we have no clear explanation for the discrepancy between our results and the micropuncture results of Argent *et al.* (1986). Inevitably the initial conditions differed: our ducts contained a significant volume of luminal fluid following overnight culture while the ducts used for micropuncture were emptied prior to the start of the collection period. It is conceivable that either the stretching of the ductal epithelium or the accumulation of some factor in the duct lumen may have had a potentiatory effect on the Cl^--dependent secretory pathway. Another possibility is suggested by previous studies which revealed quantitative differences in the secretory responses of ducts from different strains of rat (Ashton *et al.* 1990). It may also be significant that our ducts were isolated from normal rats while those used for micropuncture were taken from animals fed a copper-deficient diet in order to induce acinar cell atrophy. Whatever the reason for the discrepancy, there is no question that forskolin- and secretin-evoked fluid secretion in HCO_3^--free conditions is a highly reproducible phenomenon in both mouse and rat ducts. Its dependence on Cl^- and its total abolition by bumetanide suggest that it is more than just an artefact of the preparation.

Mechanism of Cl^- secretion in mouse and rat ducts

In the absence of HCO_3^-, fluid secretion is presumably driven by active Cl^- secretion since it was totally inhibited by substitution of Cl^- with glucuronate. The sensitivity of fluid secretion to bumetanide under these conditions indicates the probable involvement of a Na^+–K^+–$2Cl^-$ cotransporter. By analogy with the Cl^--dependent secretory mechanisms that exist in salivary glands (Cook *et al.* 1994), we would predict that the function of the cotransporter is to accumulate intracellular Cl^- across the basolateral membrane, thus achieving an intracellular Cl^- concentration somewhat above its equilibrium value. When secretin causes Cl^- channels to open in the luminal membrane, the electrochemical gradient maintained by the cotransporter will drive an efflux of Cl^- into the lumen, thus generating a Cl^--rich secretion.

Our results therefore suggest that there are parallel mechanisms for Cl^- and HCO_3^- secretion in the interlobular ducts of mouse and rat pancreas. Interestingly, similar findings have previously been reported for the human Capan-1 pancreatic duct cell line (using the short-circuit current technique) where the Cl^- secretory mechanism was also sensitive to bumetanide (Cheng *et al.* 1998). While it may be dangerous to extrapolate from cell lines to native tissue, this suggests that the two parallel mechanisms may also exist in human pancreatic ducts. On the other hand, there are good reasons to suspect that the Capan-1 phenotype most closely resembles the larger interlobular ducts in the human pancreas, which are probably not the major site of fluid secretion (Burghardt *et al.* 2003).

As well as being present in Capan-1 cells, the Na^+–K^+–$2Cl^-$ cotransporter has also been observed in cultured bovine pancreatic duct cells (Cotton, 1998). Although the cotransporter has not previously been detected in the pancreatic ducts of rodents, it is known to be present in rat bile ducts (Nathanson *et al.* 1998) which, like pancreatic ducts, also secrete fluid in response to secretin stimulation.

Relative contributions of Cl^- and HCO_3^- transport in mouse and rat ducts

Our inability to block fluid secretion in the presence of HCO_3^- by combined application of bumetanide, amiloride and DIDS alerted us to that fact that the concentrations of amiloride and DIDS used in some previous guinea-pig studies (Szalmay *et al.* 2001; Hegyi *et al.* 2003) were insufficient to completely abolish HCO_3^- accumulation across the basolateral membrane in the mouse and rat ducts. This was confirmed by measurements of intracellular pH which showed that the recovery from an acid load, involving H^+ extrusion and HCO_3^- uptake across the basolateral membrane, was only partially inhibited by 300 μM amiloride and 100 μM DIDS. Because of solubility problems with higher concentrations, we explored alternative inhibitors and found 3 μM EIPA and 500 μM H_2DIDS to be substantially more effective. Although they did not completely abolish the recovery of pH_i from acid loading, perhaps because of the strong activating influence of the low pH_i on the transporters, they did completely abolish forskolin-evoked fluid secretion when applied together with bumetanide.

This combination of inhibitors therefore provided us with the tools required to assess the relative contributions of Cl^- and HCO_3^- secretion under physiological conditions, i.e. during sustained secretion in the presence of HCO_3^-. The effects of acute exposure to the inhibitors (summarized in Fig. 7*B*) suggest that, in both the mouse and rat ducts, bumetanide-sensitive Cl^- secretion and EIPA + H_2DIDS-sensitive HCO_3^- secretion contribute almost equally to forskolin-evoked fluid secretion. This is in contrast to the guinea-pig pancreatic ducts where 10 μM *N*-methyl-*N*-isobutylamiloride (MIA) and 500 μM H_2DIDS completely abolished secretion under similar conditions (Ishiguro *et al.* 1998) and thus failed to reveal any evidence for the involvement of a basolateral Na^+–K^+–$2Cl^-$ cotransporter.

It is perhaps worth noting that Cl^- secretion could also be supported by parallel activity of the basolateral Na^+–H^+ and Cl^-–HCO_3^- exchangers as previously proposed for bombesin-stimulated secretion in the rat ducts (Ashton *et al.* 1991). Alternatively, it could be achieved by parallel activity of the basolateral Na^+–HCO_3^- cotransporter and Cl^-–HCO_3^- exchanger. Either way, this would be seen as part of the HCO_3^--dependent component of secretion and would be inhibited by EIPA (or MIA) and H_2DIDS.

One puzzling result of this study is our observation that chronic exposure to bumetanide had little effect on the forskolin-evoked secretory rate achieved in the presence of HCO_3^-. This was true for both mouse (Fig. 3*B*) and rat (Fig. 4*B*). Indeed, the secretory rate was actually enhanced, in both species, when HCO_3^- was first introduced in the presence of bumetanide. The most likely explanation is that this experimental protocol severely depleted intracellular Cl^-. In the absence of HCO_3^-, the application of bumetanide followed by forskolin will have resulted in a loss of Cl^- through apical Cl^- channels with no compensatory uptake of Cl^- across the basolateral membrane. Forskolin stimulation will also have activated the basolateral NHE1 and NBC1 transporters, so we would anticipate a rapid uptake and secretion of HCO_3^- when CO_2 and HCO_3^- were finally introduced into the bath. Although the pattern of the subsequent changes in secretory rate differed slightly between the mouse and rat ducts, both showed a decline after the initial enhancement. Nonetheless, these experiments reveal the capacity of one basolateral transport pathway – in this case the EIPA + H_2DIDS-sensitive component – to increase its activity when another – the bumetanide-sensitive component – is chronically inhibited. However, in determining the relative contributions of the two pathways to steady-state secretion, we would argue that the acute effects of the inhibitors shown in Fig. 7 probably provide a better guide.

Species differences in secreted HCO_3^- concentration

The existence of two parallel, secretin-stimulated secretory mechanisms in rat and mouse, but only one in the guinea-pig, may account for the contrasting patterns of pancreatic HCO_3^- secretion in these species. In the rat, the maximum HCO_3^- concentration in the pancreatic juice is about 70 mM (Sewell & Young, 1975), presumably because the secretion of HCO_3^- is 'diluted' by the parallel secretion of Cl^-, whereas in the guinea-pig, the maximum HCO_3^- concentration is close to 150 mM (Padfield *et al.* 1989), presumably because secretin only stimulates HCO_3^- secretion. Put another way, the guinea-pig ducts fail to secrete significant amounts of Cl^- probably because they lack the basolateral mechanisms required to sustain a driving force for Cl^- secretion across the luminal membrane. This would be consistent with previous studies of guinea-pig ducts showing that the intracellular Cl^- concentration drops to a very low level during maximal stimulation (Ishiguro *et al.* 2002*a*). The most likely explanation is that the guinea-pig duct cells lack a basolateral NKCC1 or, if present, that it is, or becomes, inactive during secretion. We already know that the basolateral anion exchanger, which could also provide a pathway for Cl^- uptake, is much reduced in activity during maximal stimulation (Ishiguro *et al.* 2000).

Similar ideas have been developed in recent studies of Calu-3 cells, an HCO_3^- and Cl^- secreting cell line derived from the submucosal glands of the human lung (Devor *et al.* 1999; Cuthbert *et al.* 2003). In these cells, Cl^- and HCO_3^- are thought to share the same apical efflux pathway, namely CFTR, but the relative rates of Cl^- and HCO_3^- secretion depend on the relative activities of the alternative basolateral uptake pathways, which vary according to the nature of the secretagogue.

In summary, our studies on fluid secretion in mouse and rat pancreatic ducts suggest that parallel secretory pathways for HCO_3^- and Cl^- are jointly responsible for fluid secretion in these species. By contrast, only the HCO_3^- secretory pathway seems to be present, or active, in guinea-pig pancreatic ducts.

Appendix

Calculation of relative volume

In this study, fluid secretory rate in isolated pancreatic duct segments has been estimated from the rate of increase in the volume of the duct lumen. The analysis of duct images obtained by video microscopy provides measurements of the image area A corresponding to the duct lumen. Values of A are first normalized with respect to the image area A_0 at the beginning of the series. To translate the resulting relative area measurements ($A_R = A/A_0$) into values for the relative luminal volume ($V_R = V/V_0$) assumptions have to be made about the geometry of the duct segments and about the way in which the lumen expands.

If we assume that the lumen of a pancreatic duct segment may be approximated by a cylinder of length l and radius r, then the image area A and the volume V are related to l and r as follows:

$$A = 2rl \tag{1}$$

$$V = \pi\, r^2 l = \frac{\pi\, A^2}{4l} \tag{2}$$

The relative area A_R and relative volume V_R are therefore given by:

$$A_R = \frac{A}{A_0} = \frac{rl}{r_0 l_0} \tag{3}$$

$$V_R = \frac{V}{V_0} = \frac{r^2 l}{r_0^2 l_0} \tag{4}$$

If the duct lumen expands by increasing in radius rather than length (so $l/l_0 = 1$), then:

$$V_R = \left(\frac{r}{r_0}\right)^2 = A_R^2 \tag{5}$$

If it expands by increasing in length rather than radius (so $r/r_0 = 1$), then:

$$V_R = \frac{l}{l_0} = A_R \tag{6}$$

If length and radius increase in proportion (so $l/l_0 = r/r_0$), then:

$$V_R = \left(\frac{r}{r_0}\right)^3 = A_R^{1.5} \tag{7}$$

Our measurements have shown that ducts vary in the relative changes in length and radius that occur as they expand, and the normal situation usually involves changes in both variables. To allow for this, the following more general relationship can be used:

$$V_R = A_R^k \tag{8}$$

An appropriate value for k may then be determined for each duct by measuring A and l in the first image of the series, and in another image selected from the series which shows the largest change in luminal volume. If the values obtained from the selected image are A_n and l_n, then from eqn (2) we get:

$$\frac{V_n}{V_0} = \frac{\left(A_n/A_0\right)^2}{l_n/l_0} \tag{9}$$

and from eqn (8) we get:

$$k = \frac{\log\left(V_n/V_0\right)}{\log\left(A_n/A_0\right)} \tag{10}$$

Substituting eqn (9) into eqn (10) gives an expression for k which can be calculated using the area and length measurements from the two images:

$$k = 2 - \frac{\log\left(l_n/l_0\right)}{\log\left(A_n/A_0\right)} \tag{11}$$

The full set of relative area data can then be transformed to relative volumes using this value for k. This still makes the assumption that the radius and length increase in a fixed proportion throughout the experiment but it obviates the need for time-consuming measurements on every image.

Calculation of secretory rate

The flow of fluid into the lumen of an isolated duct segment can be estimated from the rate of change of relative volume using:

$$\frac{dV}{dt} = V_0 \frac{dV_R}{dt} \tag{12}$$

where V_0 is obtained from the initial area and length measurements A_0 and l_0 using eqn (2):

$$V_0 = \frac{\pi A_0^2}{4l_0} \quad (13)$$

In order to express secretory rate as the volume flow per unit area of epithelium, the luminal surface area of the epithelium E is calculated using:

$$E = 2\pi r_0 l_0 = \pi A_0 \quad (14)$$

For simplicity, this calculation ignores the area corresponding to the end surfaces of the cylinder. In general the l/r ratio of the ducts is large so the contributions of the end surfaces can safely be neglected.

Therefore, combining eqns (12), (13) and (14), we can calculate the secretory rate per unit area of epithelium J_v from the rate of change of relative volume and the initial values of the image area and the duct length using:

$$J_v = \frac{A_0}{4l_0} \cdot \frac{dV_R}{dt} \quad (15)$$

References

Argent BE, Arkle S, Cullen MJ & Green R (1986). Morphological, biochemical and secretory studies on rat pancreatic ducts maintained in tissue culture. *Q J Exp Physiol* **71**, 633–648.

Ashton N, Argent BE & Green R (1990). Effect of vasoactive intestinal peptide, bombesin and substance P on fluid secretion by isolated rat pancreatic ducts. *J Physiol* **427**, 471–482.

Ashton N, Argent BE & Green R (1991). Characteristics of fluid secretion from isolated rat pancreatic ducts stimulated with secretin and bombesin. *J Physiol* **435**, 533–546.

Ashton N, Evans RL, Elliott AC, Green R & Argent BE (1993). Regulation of fluid secretion and intracellular messengers in isolated rat pancreatic ducts by acetylcholine. *J Physiol* **471**, 549–562.

Burghardt B, Elkjær ML, Kwon TH, Rácz GZ, Varga G, Steward MC & Nielsen S (2003). Distribution of aquaporin water channels AQP1 and AQP5 in the ductal system of human pancreas. *Gut* **52**, 1008–1016.

Case RM & Argent BE (1993). Pancreatic duct secretion: control and mechanisms of transport. In *The Pancreas: Biology, Pathobiology, and Disease*, ed. Go VLW, DiMagno EP, Gardner JD, Lebenthal E, Reber, HA & Scheele GA, pp. 301–350. Raven Press, New York.

Cheng HS, Leung PY, Chew SBC, Leung PS, Lam SY, Wong WS, Wang ZD & Chan HC (1998). Concurrent and independent HCO_3^- and Cl^- secretion in a human pancreatic duct cell line (CAPAN-1). *J Membr Biol* **164**, 155–167.

Cook DI, Van Lennep EW, Roberts ML & Young JA (1994). Secretion by the major salivary glands. In *Physiology of the Gastrointestinal Tract*, ed. Johnson LR, pp. 1061–1117. Raven Press, New York.

Cotton CU (1998). Ion transport properties of cultured bovine pancreatic duct epithelial cells. *Pancreas* **17**, 247–255.

Cuthbert AW, Supuran CT & MacVinish LJ (2003). Bicarbonate-dependent chloride secretion in Calu-3 epithelia in response to 7,8-benzoquinoline. *J Physiol* **551**, 79–92.

Devor DC, Singh AK, Lambert LC, DeLuca A, Frizzell RA & Bridges RJ (1999). Bicarbonate and chloride secretion in Calu-3 human airway epithelial cells. *J General Physiol* **113**, 743–760.

Gray MA, Plant S & Argent BE (1993). cAMP-regulated whole cell chloride currents in pancreatic duct cells. *Am J Physiol* **264**, C591–C602.

Gray MA, Winpenny JP, Porteous DJ, Dorin JR & Argent BE (1994). CFTR and calcium-activated chloride currents in pancreatic duct cells of a transgenic CF mouse. *Am J Physiol* **266**, C213–C221.

Greeley T, Shumaker H, Wang Z, Schweinfest CW & Soleimani M (2001). Downregulated in adenoma and putative anion transporter are regulated by CFTR in cultured pancreatic duct cells. *Am J Physiol* **281**, G1301–G1308.

Hegyi P, Gray MA & Argent BE (2003). Substance P inhibits bicarbonate secretion from guinea pig pancreatic ducts by modulating an anion exchanger. *Am J Physiol* **285**, C268–C276.

Ishiguro H, Naruse S, Kitagawa M, Mabuchi T, Kondo T, Hayakawa T, Case RM & Steward MC (2002*a*). Chloride transport in microperfused interlobular ducts isolated from guinea-pig pancreas. *J Physiol* **539**, 175–189.

Ishiguro H, Naruse S, Kitagawa M, Suzuki A, Yamamoto A, Hayakawa T, Case RM & Steward MC (2000). CO_2 permeability and bicarbonate transport in microperfused interlobular ducts isolated from guinea-pig pancreas. *J Physiol* **528**, 305–315.

Ishiguro H, Naruse S, Steward MC, Kitagawa M, Ko SBH, Hyakawa T & Case RM (1998). Fluid secretion in interlobular ducts isolated from guinea-pig pancreas. *J Physiol* **511**, 407–422.

Ishiguro H, Steward MC, Lindsay ARG & Case RM (1996). Accumulation of intracellular HCO_3^- by Na^+–HCO_3^- cotransport in interlobular ducts from guinea-pig pancreas. *J Physiol* **495**, 169–178.

Ishiguro H, Steward MC, Sohma Y, Kubota T, Kitagawa M, Kondo T, Case RM, Hayakawa T & Naruse S (2002*b*). Membrane potential and bicarbonate secretion in isolated interlobular ducts from guinea-pig pancreas. *J General Physiol* **120**, 617–628.

Kanno T & Yamamoto M (1977). Differentiation between the calcium-dependent effects of cholecystokinin-pancreozymin and the bicarbonate-dependent effects of secretin in exocrine secretion of the rat pancreas. *J Physiol* **264**, 787–799.

Ko SBH, Shcheynikov N, Choi JY, Luo X, Ishibashi K, Thomas PJ, Kim JY, Kim KH, Lee MG, Naruse S & Muallem S (2002). A molecular mechanism for aberrant CFTR-dependent HCO_3^- transport in cystic fibrosis. *EMBO J* **21**, 5662–5672.

Lee MG, Choi JY, Luo X, Strickland E, Thomas PJ & Muallem S (1999). Cystic fibrosis transmembrane conductance regulator regulates luminal Cl^-/HCO_3^- exchange in mouse submandibular and pancreatic ducts. *J Biol Chem* **274**, 14670–14677.

Linsdell P, Tabcharani JA, Rommens JM, Hou YX, Chang XB, Tsui LC, Riordan JR & Hanrahan JW (1997). Permeability of wild-type and mutant cystic fibrosis transmembrane conductance regulator chloride channels to polyatomic anions. *J General Physiol* **110**, 355–364.

Lohi H, Kujala M, Kerkela E, Saarialho-Kere U, Kestila M & Kere J (2000). Mapping of five new putative anion transporter genes in human and characterization of SLC26A6, a candidate gene for pancreatic anion exchanger. *Genomics* **70**, 102–112.

Mangos JA, McSherry NR, Nousia-Arvanitakis S & Irwin K (1973). Secretion and transductal fluxes of ions in exocrine glands of the mouse. *Am J Physiol* **225**, 18–24.

Nathanson MH, Burgstahler AD, Mennone A, Dranoff JA & Rios-Velez L (1998). Stimulation of bile duct epithelial secretion by glibenclamide in normal and cholestatic rat liver. *J Clin Invest* **101**, 2665–2676.

O'Reilly CM, Winpenny JP, Argent BE & Gray MA (2000). Cystic fibrosis transmembrane conductance regulator currents in guinea pig pancreatic duct cells: Inhibition by bicarbonate ions. *Gastroenterol* **118**, 1187–1196.

Padfield PJ, Garner A & Case RM (1989). Patterns of pancreatic secretion in the anaesthetised guinea pig following stimulation with secretin, cholecystokinin octapeptide, or bombesin. *Pancreas* **4**, 204–209.

Petersen OH & Ueda N (1977). Secretion of fluid and amylase in the perfused rat pancreas. *J Physiol* **264**, 819–835.

Poulsen JH, Fischer H, Illek B & Machen TE (1994). Bicarbonate conductance and pH regulatory capability of cystic fibrosis transmembrane conductance regulator. *Proc Natl Acad Sci U S A* **91**, 5340–5344.

Sewell WA & Young JA (1975). Secretion of electrolytes by the pancreas of the anaesthetized rat. *J Physiol* **252**, 379–396.

Shumaker H & Soleimani M (1999). CFTR upregulates the expression of the basolateral Na^+-K^+-$2Cl^-$ cotransporter in cultured pancreatic duct cells. *Am J Physiol* **277**, C1100–C1110.

Sohma Y, Gray MA, Imai Y & Argent BE (2000). HCO_3^- transport in a mathematical model of the pancreatic ductal epithelium. *J Membr Biol* **176**, 77–100.

Szalmay G, Varga G, Kajiyama F, Yang XS, Lang TF, Case RM & Steward MC (2001). Bicarbonate and fluid secretion evoked by cholecystokinin, bombesin and acetylcholine in isolated guinea-pig pancreatic ducts. *J Physiol* **535**, 795–807.

Thomas JA, Buchsbaum RN, Zimniak A & Racker E (1979). Intracellular pH measurements in Ehrlich ascites tumor cells utilizing spectroscopic probes generated in situ. *Biochemistry* **18**, 2210–2218.

Xie Q, Welch R, Mercado A, Romero MF & Mount DB (2002). Molecular characterization of the murine SLC26A6 anion exchanger: functional comparison with SLC26A1. *Am J Physiol* **283**, F826–F838.

Zhao H, Star RA & Muallem S (1994). Membrane localization of H^+ and HCO_3^- transporters in the rat pancreatic duct. *J General Physiol* **104**, 57–85.

Acknowledgements

This study was funded by the Cystic Fibrosis Trust (UK), the Wellcome Trust and the DGICYT (Spain; project number PB1998-0274). J.I.S.R. was a Wellcome Trust Travelling Research Fellow.